

An Analysis of Diagonal and Non-diagonal QCD Sum Rules for Heavy Baryons at Next-to-Leading Order in α_S

S. Groote,¹ J.G. Körner²

Institut für Physik, Johannes-Gutenberg-Universität,
Staudinger Weg 7, D-55099 Mainz, Germany

O.I. Yakovlev³

Institut für theoretische Physik II,
Bayrische Julius-Maximilians-Universität,
Am Hubland, D-97074 Würzburg, Germany

Abstract

We consider diagonal and non-diagonal QCD sum rules for the ground state heavy baryons to leading order in $1/m_Q$ and at next-to-leading order in α_S . In the non-diagonal case we evaluate the eight different two-loop diagrams which determine the perturbative α_S -corrections to the Wilson coefficient of the quark condensate in the Operator Product Expansion. The QCD corrections to the non-diagonal sum rules are moderate compared to the QCD corrections in the diagonal case. We also consider constituent type sum rules using constituent type interpolating currents. The obtained results are in reasonable agreement with the corresponding results obtained in the diagonal case. As central values for the bound state energies we find $m(\Lambda_Q) - m_Q \simeq 760 \text{ MeV}$ and $m(\Sigma_Q) - m_Q \simeq 940 \text{ MeV}$. The central values for the residues are given by $F(\Lambda_Q) \simeq 0.030 \text{ GeV}^3$ and $F(\Sigma_Q) \simeq 0.038 \text{ GeV}^3$.

¹Groote@dipmza.physik.uni-mainz.de

²Koerner@dipmza.physik.uni-mainz.de

³O_Yakovlev@physik.uni-wuerzburg.de;

on leave from Budker Institute of Nuclear Physics (BINP),
pr. Lavrenteva 11, Novosibirsk, 630090, Russia

1 Introduction

The knowledge of the non-perturbative properties of heavy hadrons such as their binding energies or their weak transition matrix elements are of fundamental importance for the determination of the fundamental parameters of the Standard Model. Among these are the quark masses and the values of the Cabibbo-Kobayashi-Maskawa matrix elements. A convenient access to the properties of heavy hadrons containing one heavy quark is given by the Heavy Quark Effective Theory (HQET) which provides a systematic power series expansion of physical matrix elements involving heavy hadrons in terms of the inverse of the heavy quark mass (see for example [1]). While the case of heavy meson systems has been analyzed in great detail, corresponding calculations for heavy baryon systems have been lagging behind. This is unfortunate since results from the analysis of heavy baryon systems are expected to provide important supplementary information on the non-perturbative dynamics of QCD and on the fundamental parameters of the Standard Model. The importance of further theoretical studies on heavy baryon systems is highlighted by the fact that there is now an abundance of new experimental data on heavy baryon decays sparked by recent advances in microvertexing techniques. This data needs to be analyzed and interpreted theoretically.

A convenient and well-trusted tool to investigate the non-perturbative properties of heavy hadrons is the QCD sum rule method [2]. The first application of the QCD sum rule method to heavy baryons was considered some time ago by Shuryak [3] who studied heavy baryons in the static limit given by the leading term in the $1/m_Q$ expansion. The work of Shuryak [3] was revised and extended in [4, 5]. An analysis of heavy baryons containing large but finite quark masses m_Q was undertaken in [6, 7, 8].

We have recently been embarking on a program to improve on previous analysis of heavy baryon sum rules by including first order radiative corrections in the analysis. In [9] we determined the two-loop anomalous dimensions of the static heavy baryon currents. In [10] we determined the perturbative α_S corrections to the leading, dimension zero, term in the operator product expansion (OPE) of the static heavy baryon current correlator. Similar to the heavy meson case investigated e.g. in [11, 12] the radiative corrections to the perturbative dimension zero term are quite large. The results of [9, 10] were used to construct and analyze so-called diagonal QCD sum rules for heavy baryons [10].

Here the term “diagonal” refers to a particular feature of heavy baryon currents and their current products. For every baryonic state there are two independent interpolating currents even in the static limit [3, 4, 9]. One can thus construct diagonal sum rules from current correlators of the same baryon current and non-diagonal sum rules from current correlators of different baryon currents. The structure of the sum rules for the two cases is qualitatively quite different. Nevertheless, they must be considered on the same footing. In [10] we provided a detailed analysis of the diagonal sum rules. The main part of the present paper is devoted to an analysis of the non-diagonal sum rules including radiative corrections. We compare our results with those obtained from the analysis of the diagonal sum rules. Using results from [10] we also analyze mixed sum rules where we use constituent type current combinations in the current correlators.

In order to provide a brief synopsis of the structural differences of the diagonal and non-diagonal sum rules let us briefly recapitulate the main features of the diagonal sum rule analysis [3, 4, 10]:

- QCD sum rules based on diagonal correlators feature a leading order spectral density

which grows rapidly with energy as $\rho(\omega) \sim \omega^5$. This rapid growth introduces a strong dependence of the results on the assumed value of the continuum threshold.

- The QCD radiative correction to the leading order spectral density amounts to about 100% at the renormalization scale $\mu = 1 \text{ GeV}$.
- Despite of the large QCD corrections to the Wilson coefficients in the OPE, the lowest order sum rules and the radiatively corrected sum rules predict nearly the same values for the masses and the residues, while the stability region of the sum rule results appears at slightly shifted values of the continuum threshold.

It is clear that one also needs to analyze the non-diagonal sum rules in addition to the diagonal sum rules if only for reasons of consistency. A welcome property of the non-diagonal correlator is the quite “normal” behaviour $\rho(\omega) \sim \omega^2$ of the spectral density and the fact that the QCD corrections are moderate.

The paper is organized as follows. In Sect. 2 we introduce our notation and construct the correlator of two heavy baryon currents. We also recall the form of the known QCD corrections to the dimension zero term of the OPE. In Sect. 3 we present our results on the QCD corrections to the dimension three contribution in the OPE, which is proportional to the vacuum expectation value of the product of the quark and the antiquark field. We also construct generalized QCD sum rules which incorporate both the diagonal and the non-diagonal case. Sect. 4 contains the results of our numerical analysis, our final numbers and a discussion of the results. In an Appendix we collect our results on the evaluation of the radiative two-loop corrections to the dimension-three condensate contribution. The results are given for D -dimensional space-time using the most general baryon current structure.

2 Correlator of two baryonic currents

2.1 Basic notions

In this section we briefly recapitulate the basic notions involved in the construction of QCD sum rules for heavy baryons. This also serves to introduce our notation which closely follows the one used in [9, 10]. The starting point is given by the correlator of two baryonic currents ($i, j = 1, 2$)

$$\Pi_{ij}(\omega = k \cdot v) = i \int d^4x e^{ikx} \langle 0 | T \{ J_i(x), \bar{J}_j(0) \} | 0 \rangle, \quad (1)$$

where k_μ is the residual momentum of the heavy quark and v_μ is the four-velocity of the heavy baryon, the product of both being denoted by ω . The residual momentum and the four-velocity are related by $p_\mu = m_Q v_\mu + k_\mu$, where p_μ denotes the momentum of the heavy quark and m_Q is its mass. As was mentioned before, there are two possible choices of interpolating currents for each of the heavy baryon states. Neglecting the flavour and colour structure for the moment, these are given by⁴

$$J_1 = [q^T C \Gamma_1 q] \Gamma' Q \quad \text{and} \quad J_2 = [q^T C \Gamma_2 q] \Gamma' Q, \quad (2)$$

⁴Here we use a rather symbolic notation. The Dirac strings Γ and Γ' can carry Lorentz indices. A contraction on the Lorentz indices is always implied when writing the currents in the form of Eq. (2)

Γ	n	s	particles
γ_5	0	+1	Λ_1
$\gamma_5\gamma_0$	1	-1	Λ_2
$\vec{\gamma}$	1	+1	Σ_1, Σ_1^*
$\gamma_0\vec{\gamma}$	2	-1	Σ_2, Σ_2^*

Table 1: Specific values of the parameter pair (n, s) for particular cases of the light-side Dirac structure Γ .

where

$$\Gamma_1 = \Gamma \quad \text{and} \quad \Gamma_2 = \Gamma\psi. \quad (3)$$

To be more precise, it is clear that the multiplication of the light-side Dirac structure Γ with ψ does not change the quantum numbers of the interpolating current but does change the structure of the current. Multiplying the heavy-side structure Γ' with ψ , however, does not change the structure of the interpolating current since $\psi Q = Q$ in the static limit.

In the static limit one has two types of heavy ground state baryons depending on whether the light diquark system is in a spin 0 or in a spin 1 state. We shall employ a generic notation and refer to the first type (spin 0 diquark) as Λ_Q -type heavy baryons. The Dirac structure of the interpolating current is given by $\Gamma = \gamma_5$ and $\Gamma' = 1$ in this case. In the second case (spin 1 diquark) one has a doublet of degenerate Σ_Q -type states with overall spin 1/2 and 3/2. For the spin 1/2 Σ_Q -type state the interpolating current is given by $\Gamma = \gamma_\perp^\mu \equiv \gamma^\mu - \psi v^\mu$ and $\Gamma' = \gamma_\perp^\mu \gamma_5$. The explicit form of the spin 3/2 interpolating current (Σ_Q^* -type state) can be found e.g. in [10].

For a general analysis it proves convenient to represent the general light-side Dirac structure of the currents in Eq. (2) by an antisymmetrized product of n Dirac matrices $\Gamma = \gamma^{[\mu_1} \dots \gamma^{\mu_n]}$. When calculating the one- and two-loop vertex corrections to the baryon currents in Eq. (2) one encounters γ -contractions of the form $\gamma_\alpha \Gamma \gamma^\alpha$ and $\psi \Gamma \psi$. The γ_α -contraction leads to an n -dependence according to

$$\gamma_\alpha \Gamma \gamma^\alpha = (-1)^n (D - 2n) \Gamma, \quad (4)$$

where D denotes the space-time dimension. The ψ -contraction depends in addition on the parameter s which takes the value $(s = +1)$ and $(s = -1)$ for an even or odd number of ψ 's in Γ , respectively. The ψ -contraction reads

$$\psi \Gamma \psi = (-1)^n s \Gamma. \quad (5)$$

Some of our results in the next sections are given in terms of the most general Dirac structure of heavy baryon currents involving the parameters n and s whose definitions should be kept in mind. For the convenience of the reader we list the relevant (n, s) -values for the cases studied in this paper in Table 1.

2.2 Anomalous dimensions of heavy baryon currents

The one-loop and two-loop renormalization of the static heavy baryon currents and their anomalous dimensions were considered in [4] and [9], respectively. Note that the anomalous dimensions of the currents differ in general from those in conventional QCD. We

define the anomalous dimensions in terms of the expansion $\gamma = \sum_k (\alpha_S/4\pi)^k \gamma_k$. The one-loop anomalous dimension for the general current case depends only on the parameter n which specifies the light-side Dirac structure. The one-loop anomalous dimension is given by [4, 9]

$$\gamma_1 = -\frac{4}{3}((n-2)^2 + 2). \quad (6)$$

The general (n, s) -dependent formula for the two-loop anomalous dimension case is rather lengthy and will therefore not be listed here. The general formula can be found in [9]. Here we specify to the case of the heavy ground state baryons and give the expansion to two-loop order using the $\overline{\text{MS}}$ -scheme and a naively anticommuting γ_5 . One has

$$\gamma_{\Lambda 1} = -8 \left(\frac{\alpha_S}{4\pi} \right) + \underbrace{\frac{1}{9}(16\zeta(2) + 40N_f - 796)}_{\approx -72.19} \left(\frac{\alpha_S}{4\pi} \right)^2, \quad (7)$$

$$\gamma_{\Lambda 2} = -4 \left(\frac{\alpha_S}{4\pi} \right) + \underbrace{\frac{1}{9}(16\zeta(2) + 20N_f - 322)}_{\approx -26.19} \left(\frac{\alpha_S}{4\pi} \right)^2, \quad (8)$$

$$\gamma_{\Sigma 1} = -4 \left(\frac{\alpha_S}{4\pi} \right) + \underbrace{\frac{1}{9}(16\zeta(2) + 20N_f - 290)}_{\approx -22.63} \left(\frac{\alpha_S}{4\pi} \right)^2, \quad (9)$$

$$\gamma_{\Sigma 2} = -\frac{8}{3} \left(\frac{\alpha_S}{4\pi} \right) + \underbrace{\frac{1}{27}(48\zeta(2) + 8N_f + 324)}_{\approx 15.81} \left(\frac{\alpha_S}{4\pi} \right)^2, \quad (10)$$

where the numerical values are given for the case of three light flavours ($N_f = 3$).

3 Diagonal, non-diagonal and mixed correlators

As mentioned before, the two independent currents give rise to two independent types of correlators, namely the diagonal correlators $\langle J_1 \bar{J}_1 \rangle$ and $\langle J_2 \bar{J}_2 \rangle$, and the non-diagonal correlators $\langle J_1 \bar{J}_2 \rangle$ and $\langle J_2 \bar{J}_1 \rangle$. In the general case, one may even consider correlators built from a linear combination $J = aJ_1 + (1-a)J_2$ of currents with an arbitrary coefficient a ($0 \leq a \leq 1$). We shall, however, not discuss the most general linear combination of currents in this paper. Later on we investigate the case $a = 1/2$. The choice $J = (J_1 + J_2)/2$ corresponds to a constituent quark model current which has maximal overlap with the ground state baryons in the constituent quark model picture.

Following the standard QCD sum rule method [2], the correlator is calculated in the Euclidean region $-\omega \approx 1 - 2 \text{ GeV}$ including perturbative and non-perturbative contributions. In the Euclidean region the non-perturbative contributions are expected to form a convergent series. The non-perturbative effects are taken into account by employing an OPE for the time-ordered product of the currents in Eq. (1). One then has

$$\begin{aligned} \langle T\{J(x), \bar{J}(0)\} \rangle &= \sum_d C_d(x^2) O_d \\ &= C_0(x^2) O_0 + C_3(x^2) O_3 + C_4(x^2) O_4 + C_5(x^2) O_5 + \dots \end{aligned} \quad (11)$$

where the O_d are vacuum expectation values of local operators whose dimensions are labelled by their subscripts d . $O_0 = \hat{1}$ corresponds to the so called perturbative term,

$O_3 = \langle \bar{q}q \rangle$ is a quark condensate term, $O_4 = \alpha_S \langle G^2 \rangle$ is a gluon condensate term, $O_5 = g_S \langle \bar{q} \sigma_{\mu\nu} G^{\mu\nu} q \rangle$ is a mixed quark-gluon condensate, and so on. The expansion coefficients $C_d(x^2)$ are the associated coefficient functions or Wilson coefficients of the OPE.

A straightforward dimensional analysis shows that the OPE of the diagonal correlators $\langle J_1 \bar{J}_1 \rangle$ and $\langle J_2 \bar{J}_2 \rangle$ contains only even-dimensional terms, while the OPE of the non-diagonal correlators contains only odd-dimensional terms. This classification is preserved when radiative corrections are included, assuming the light quarks to be massless. We apply radiative corrections only to the leading terms in the OPE because the non-leading contributions are small.

The diagonal case was studied in detail in [10]. It was shown that the QCD corrections to the spectral density of the correlator function $P(\omega)$ are quite large. It is quite intriguing that the contributions of the four different three-loop diagrams that contribute to the perturbative dimension zero piece shown in Fig. 1 can be collected into one compact formula [10]:

$$\frac{\rho_0^{\text{QCD}}(\omega, \mu)}{\rho_0^{\text{Born}}(\omega)} = 1 + \frac{\alpha_S}{4\pi} \left[\ln \left(\frac{\mu}{2\omega} \right) \frac{8}{3} (n^2 - 4n + 6) + \frac{8}{45} (60\zeta(2) + 38n^2 - 137n + 273) \right]. \quad (12)$$

The number n specifies the light-side Dirac structure of the baryon currents as before. Note that the coefficient of the logarithmic term coincides with the one-loop anomalous dimension of the diagonal correlator which in this case is equal to two times the anomalous dimension of the baryon current itself.

3.1 Non-diagonal correlators

The non-diagonal correlator of the two heavy baryon currents reads

$$\Pi_{12}(\omega) = i \int d^4x e^{ikx} \langle 0 | T \{ J_1(x) \bar{J}_2(0) \} | 0 \rangle = \Gamma'_1 \frac{1 + \psi}{2} \bar{\Gamma}'_2 \frac{1}{4} \text{Tr}(\Gamma_1 \bar{\Gamma}_2) P_{12}(\omega). \quad (13)$$

We have suppressed the flavour and colour labels in Eq. (13). The OPE for the non-diagonal correlator contains a term $O_3(\mu) = \langle \bar{q}q \rangle$ proportional to the quark condensate, a mixed quark-gluon condensate term $O_5(\mu) = g_S \langle \bar{q} \sigma_{\mu\nu} G^{\mu\nu} q \rangle \equiv m_0^2 \langle \bar{q}q \rangle$, a term $O_7(\mu) = \langle \bar{q}q \rangle \langle \alpha_S G^2 \rangle$, and a term $O_9 = \alpha_S \langle \bar{q}q \rangle^3$. Taking into account these four condensate contributions, the Fourier transform of the scalar correlator function $P(\omega)$ is given by

$$\begin{aligned} P(t) &= P_{\text{OPE}}(t) \\ &= -i \frac{2\theta(t)}{\pi^2 t^3} \left(O_3(\mu) + \frac{t^2}{16} \left(1 - \frac{c}{2} \right) O_5(\mu) + \frac{\pi t^4}{288} \left(1 - \frac{c}{2} \right) O_7(\mu) - \frac{\pi^3 t^6}{972} O_9(\mu) \right), \end{aligned} \quad (14)$$

where c is a Clebsch-Gordan type factor which takes the values $c = 1$ for the Λ_Q -type and $c = -1/3$ for the Σ_Q -type doublet $\{\Sigma_Q, \Sigma_Q^*\}$ ground state baryons. The correlator function $P_{\text{OPE}}(\omega)$ satisfies the dispersion relation

$$P_{\text{OPE}}(\omega) = P(\omega) = \int_0^\infty \frac{\rho(\omega') d\omega'}{\omega' - \omega - i0} + \text{subtraction}, \quad (15)$$

where $\rho(\omega) = \text{Im}(P(\omega))/\pi$ is the spectral density of the scalar correlation function. Taking into account the above four condensate contributions, the lowest order spectral density of

the first two contributions is given by [4, 5]

$$\rho_3(\omega) = -\frac{\langle \bar{q}q \rangle}{\pi^2} \omega^2 \quad \text{and} \quad \rho_5(\omega) = 2 \left(1 - \frac{c}{2}\right) \frac{\langle \bar{q}q \rangle m_0^2}{16\pi^2}. \quad (16)$$

Next we compute the radiative corrections to the quark condensate term $\rho_3(\omega)$. There are altogether eight different contributing diagrams which are shown in Fig. 2. Their contributions were evaluated with the help of the algorithm developed in [15]. As a check on the calculation we used a general covariant gauge for the gluon. The gauge dependence was found to drop out in the sum of the contributions.

Collecting together the one- and two-loop contributions to the dimension three scalar correlation function one has

$$P_3(\omega) = -\frac{\langle \bar{q}q \rangle}{2\pi^2} \omega^2 \left(\left(\frac{-2\omega}{\mu} \right)^{D-4} C_0 D_0 + \frac{g_S^2}{(4\pi)^{D/2}} \left(\frac{-2\omega}{\mu} \right)^{2D-8} \sum_{i=1}^8 C_i D_i \right), \quad (17)$$

where $D = 4 - 2\epsilon$ is the space-time dimension. There are a number of colour factors in Eq. (17) the values of which are given by $C_0 = N_c!$, $C_1 = C_2 = C_3 = C_4 = C_5 = -N_c! C_B$ and $C_6 = C_7 = C_8 = N_c! C_F$, where N_c is the number of colours, $C_F = (N_c^2 - 1)/2N_c$, and $C_B = (N_c + 1)/2N_c$. Explicit forms of the scalar coefficients D_i defined in Eq. (17) are listed in Appendix A. When Eq. (17) is expanded in terms of a power series in $1/\epsilon$, one obtains

$$\begin{aligned} P_3(\omega) = & -\frac{\langle \bar{q}q \rangle}{2\pi^2} \omega^2 \left[\left(\frac{-\mu}{2\omega} \right)^{2\epsilon} \left(\frac{1}{\epsilon} + 2 \right) \right. \\ & + \frac{\alpha_S}{12\pi} \left(\frac{-\mu}{2\omega} \right)^{4\epsilon} \left(\frac{1}{\epsilon^2} (2n^2 - 8n + 7 + 2(n-2)s) \right. \\ & \quad + \frac{1}{\epsilon} (12n^2 - 44n + 51 + (12n - 22)s + 8\zeta(2)) \\ & \quad + 56n^2 - 200n + 260 + (56n - 100)s \\ & \quad \left. \left. + (18n^2 - 72n + 87 + 18s(n-2))\zeta(2) - 32\zeta(3) \right) \right], \quad (18) \end{aligned}$$

where we have now substituted explicit values for the colour factors with $N_c = 3$. The spectral density $\rho_3(\omega)$ is given by the absorptive part of $P_3(\omega)$. In renormalizing the spectral density $\rho_3(\omega)$ one has to take into account both the renormalization factor of the baryon currents [4] and the renormalization factor of the quark condensate,

$$\rho_3(\omega) = Z_{J_1} Z_{J_2} Z_{\bar{q}q}^{-1} \rho_3^{\text{ren}}(\omega) \quad (19)$$

with [10, 12]

$$\begin{aligned} Z_{\bar{q}q} &= 1 + 3 \frac{\alpha_S C_F}{4\pi\epsilon}, \\ Z_{J_1} &= 1 + \frac{\alpha_S C_B}{4\pi\epsilon} (n^2 - 4n + 6) \quad \text{and} \\ Z_{J_2} &= 1 + \frac{\alpha_S C_B}{4\pi\epsilon} ((n-2+s)^2 + 2). \quad (20) \end{aligned}$$

After multiplication with the Z -factors the leading $1/\epsilon$ -contribution in $\rho_3(\omega)$ is cancelled. The renormalized spectral density is given by

$$\rho_3^{\text{ren}}(\omega) = \rho_3^{\text{Born}}(\omega) \left[1 + \frac{\alpha_S}{4\pi} r(\omega/\mu) \right], \quad (21)$$

where

$$\rho_3^{\text{Born}}(\omega) = -\frac{\langle \bar{q}q \rangle^{\text{ren}}}{\pi^2} \omega^2 \quad \text{and} \quad r(\omega/\mu) = r_1 \ln \left(\frac{\mu}{2\omega} \right) + r_2 \quad (22)$$

with

$$\begin{aligned} r_1 &:= \frac{4}{3}(2n^2 - 8n + 7 + 2(n-2)s) \quad \text{and} \\ r_2 &:= \frac{2}{3}(8n^2 - 28n + 37 + 8ns - 14s + 8\zeta(2)). \end{aligned} \quad (23)$$

Note that the coefficient r_1 of the logarithmic term in Eq. (22) coincides with the sum of the one-loop anomalous dimension of J_1 and J_2 minus the anomalous dimension of the quark condensate. The reason is that the same coefficient is involved in the cancellations of the $1/\epsilon$ -pole in Eq. (19).

Explicit values for the correction to the spectral density for the cases of the Λ_Q - and Σ_Q -type ground state baryons are given by

$$r_\Lambda(\omega/\mu) = 4 \ln \left(\frac{\mu}{2\omega} \right) + \frac{2}{3}(23 + 8\zeta(2)) \quad (24)$$

and

$$r_\Sigma(\omega/\mu) = -\frac{4}{3} \ln \left(\frac{\mu}{2\omega} \right) + \frac{2}{3}(11 + 8\zeta(2)). \quad (25)$$

The radiative corrections can be seen to amount to about 40–60% at the renormalization scale $\mu = 1 \text{ GeV}$. Due to the hermiticity of the current correlator Π_{ij} the coefficients r_1 and r_2 do not depend on which of the two non-diagonal current products $J_1 \bar{J}_2$ or $J_2 \bar{J}_1$ are taken.

3.2 Non-diagonal sum rules

As usual we construct QCD sum rules by invoking parton-hadron duality, i.e. we equate the theoretical contribution to the scalar correlation function $P(\omega)$ given in Eq. (13) with the dispersion integral over the contributions of hadron states. These consist of the lowest lying ground state with bound state energy $\bar{\Lambda}$ plus the excited states and the continuum contributions. To leading order in $1/m_Q$ the bound state energy of the ground state is defined by

$$m_{\text{baryon}} = m_Q + \bar{\Lambda}, \quad (26)$$

where m_Q is the pole mass of the heavy quark. We assume that the contribution of the excited states and the continuum contribution sets in above some effective threshold energy E_C and can be approximated by the OPE expression [2]. For the hadron-side contribution ρ_{HS} to the spectral density we thus write

$$\rho_{\text{HS}}(\omega) = \rho_{\text{GS}}(\omega) + \rho_{\text{cont}}(\omega), \quad (27)$$

where the contribution of the lowest-lying ground state baryon is denoted by ρ_{GS} and is given by

$$\rho_{\text{GS}}(\omega) = \frac{1}{2}F_1F_2\delta(\omega - \bar{\Lambda}). \quad (28)$$

The residues F_i ($i = 1, 2$) appearing in Eq. (28) are defined by the matrix elements of the heavy baryon currents according to

$$\langle 0|J_i|\Lambda_Q\rangle = F_{i\Lambda}u, \quad \langle 0|J_i|\Sigma_Q\rangle = F_{i\Sigma}u \quad \text{and} \quad \langle 0|J'_i|\Sigma_Q^*\rangle = \frac{1}{\sqrt{3}}F_{i\Sigma^*}u', \quad (29)$$

where u and u' are the usual spin 1/2 and spin 3/2 spinors. Note that $F_{i\Sigma^*}$ coincides with $F_{i\Sigma}$ to lowest order of the heavy quark mass expansion which we are working in.

As is usual we assume hadron-parton duality for the contributions of excited states and the continuum contributions. As mentioned before we subsume these contributions by defining an effective energy threshold E_C and write $\rho_{\text{cont}}(\omega) = \theta(\omega - E_C)\rho(\omega)$, where ρ is the result of the OPE calculations given in Eqs. (16) and (21). With these assumptions we arrive at the sum rule

$$P_{\text{OPE}}(\omega) = \frac{\frac{1}{2}F_1F_2}{\bar{\Lambda} - \omega - i0} + \int_{E_C}^{\infty} \frac{\rho(\omega')d\omega'}{\omega' - \omega - i0} \quad (30)$$

or

$$\frac{\frac{1}{2}F_1F_2}{\bar{\Lambda} - \omega - i0} = \int_0^{E_C} \frac{\rho(\omega')d\omega'}{\omega' - \omega - i0} + P_{\text{PC}}(\omega). \quad (31)$$

The polynomial contribution $P_{\text{PC}}(\omega)$ is defined as the Fourier transform of that part of the correlator function $P(t)$ which contains non-negative powers $(t^2)^n$ ($n \geq 0$). Finally we apply the Borel transformation

$$\hat{B}_T = \lim_{\omega \rightarrow \infty} \frac{\omega^n}{\Gamma(n)} \left(-\frac{d}{d\omega} \right)^n \quad n, -\omega \rightarrow \infty \quad (T = -\omega/n \text{ fixed}) \quad (32)$$

to the sum rule in Eq. (31). Using $\hat{B}_T(1/(\omega - \omega')) = \exp(-\omega'/T)/T$ we obtain the Borel sum rule

$$\frac{1}{2}F_1(\mu)F_2(\mu)e^{-\bar{\Lambda}/T} = \int_0^{E_C} \rho(\omega', \mu)e^{-\omega'/T}d\omega' + \hat{B}P_{\text{PC}}(T) =: K(E_C, T, \mu), \quad (33)$$

where we have reintroduced the μ -dependence of the spectral density which in turn gives rise to a μ -dependence of the residue. The Borel-transformed polynomial contribution $\hat{B}P_{\text{PC}}(T)$ can be obtained directly from $P_{\text{PC}}(t)$ by the substitution $t \rightarrow -i/T$ (see the discussion in [4]). Note that the bound state energy $\bar{\Lambda}$ can be obtained from the sum rule in Eq. (33) by taking the logarithmic derivative with respect to the inverse Borel parameter according to

$$\bar{\Lambda} = -\frac{d \ln(K(E_C, T, \mu))}{dT^{-1}}. \quad (34)$$

Before turning to the numerical analysis of the non-diagonal sum rules we want to briefly comment on the scale dependence of the residues. The numerical values given below are taken at the specific normalization point $\mu = 1 \text{ GeV}$, while the general dependence on the scale μ is controlled by the renormalization group equation. At one-loop order the

product of the residues at one renormalization point μ_2 can be expressed by the product at another renormalization point μ_1 via

$$F_1(\mu_2)F_2(\mu_2) = F_1(\mu_1)F_2(\mu_1)U(\mu_1, \mu_2) \quad (35)$$

with

$$U(\mu_1, \mu_2) = \left(\frac{\alpha_S(\mu)}{\alpha_S(\mu_0)} \right)^{\gamma_1/\beta_1}, \quad (36)$$

where $U(\mu_1, \mu_2)$ is the evolution function which takes one from the scale μ_2 to the scale μ_1 . The coefficients $\beta_1 = 11 - 2/3N_c$ and γ_1 are the usual first-order terms in the expansion of the QCD β -function and the anomalous dimension $\gamma_P = \gamma_{J_1} + \gamma_{J_2} - \gamma_{\bar{q}q}$ of the non-diagonal scalar correlator function P . The two-loop extension of Eq. (36) is given by

$$\begin{aligned} U(\mu_1, \mu_2) &= \exp \left(\int_{\alpha_S(\mu_2)}^{\alpha_S(\mu_1)} \frac{d\alpha}{\alpha} \frac{\gamma(\alpha)}{\beta(\alpha)} \right) \\ &= \left(\frac{\alpha_S(\mu_1)}{\alpha_S(\mu_2)} \right)^{\gamma_1/\beta_1} \left(1 + \frac{\alpha_S(\mu_1) - \alpha_S(\mu_2)}{4\pi} \frac{\gamma_1}{\beta_1} \left(\frac{\gamma_2}{\gamma_1} - \frac{\beta_2}{\beta_1} \right) \right), \end{aligned} \quad (37)$$

where β_n is the n -th order term in the β -function expansion and γ_n denotes the anomalous dimension of the non-diagonal scalar correlator function P at n -th loop order. The two-loop evolution function in Eq. (37) is obtained as a solution to the renormalization group equation including next-to-leading order perturbative terms in α_S (see also the discussion in [11, 12, 13, 14]).

It is evident that we can only extract the value of the product of residues F_1F_2 from our sum rule analysis. In order to make further progress, we adopt the working hypothesis that the residues of the two current options in each case are equal. This assumption is corroborated by the results of the diagonal sum rule analysis [10]. This means we replace F_1F_2 by F^2 in the above formulae when performing the numerical analysis. We note, however, that the currents J_1 and J_2 have different anomalous dimensions and therefore F_1 and F_2 do not coincide at another renormalization scale μ_2 even if they coincide at the scale μ_1 . Returning to the sum rule in Eq. (33), one then has

$$\begin{aligned} \frac{1}{2}F^2(\mu)e^{-\bar{\Lambda}/T} &= \frac{2N_c!}{\pi^4} \left[E_Q^3 T^3 \left(f_2(x_C) + \frac{\alpha_S}{4\pi} \left(\left(\ln \left(\frac{\mu}{2T} \right) f_2(x_C) - f_2^l(x_C) \right) r_1 + f_2(x_C) r_2 \right) \right) \right. \\ &\quad \left. - E_Q^3 E_0^2 T \left(1 - \frac{c}{2} \right) f_0(x_C) + \frac{2}{3} \left(1 - \frac{c}{2} \right) \frac{E_Q^3 E_G^4}{T} + \frac{\alpha_S C_F E_Q^9}{36\pi T^3} \right], \end{aligned} \quad (38)$$

where the (n, s) -dependent coefficient functions r_1 and r_2 are defined in Eq. (23) and the functions f_n and f_n^l are given by

$$\begin{aligned} f_n(x) &:= \int_0^x \frac{x'^n}{n!} e^{-x'} dx' = 1 - e^{-x} \sum_{m=0}^n \frac{x^m}{m!}, \\ f_n^l(x) &:= \int_0^x \frac{x'^n}{n!} \ln x' e^{-x'} dx'. \end{aligned} \quad (39)$$

In order to simplify the notation we have introduced the abbreviations

$$x_C := \frac{E_C}{T}, \quad E_0 := \frac{m_0}{4}, \quad (E_Q)^3 := -\frac{\pi^2}{2N_c} \langle \bar{q}q \rangle \quad \text{and} \quad (E_G)^4 := \frac{\pi \alpha_S \langle G^2 \rangle}{32N_c(N_c - 1)}. \quad (40)$$

3.3 Mixed sum rules of constituent type

As mentioned before, we shall not investigate the most general case of mixed sum rules but specify to the linear combination of currents $J = (J_1 + J_2)/2$ in the sum rules. The light-side Dirac structure of the currents can then be seen to appear in the form $\frac{1}{2}(1 + \psi)\Gamma$, i.e. one has the projector factor $P_+ = (1 + \psi)/2$ which projects on the large components of the light quark fields. In the rest system of the heavy baryon, where $v_\mu = (1; 0, 0, 0)$, this is manifest since then $P_+ = \begin{pmatrix} 1 & 0 \\ 0 & 0 \end{pmatrix}$. We refer to this particular linear combination of currents as the constituent type current. This linear combination of currents is expected to have maximum overlap with the heavy ground state baryons in the constituent quark model, i.e. where the light diquark state in the heavy baryon is taken to be composed of on-shell light quarks. We mention that the constituent quark model picture emerges in the large N_c -limit [16]. The tools needed for the sum rule analysis of constituent type heavy baryons have been assembled in this paper and in [9]. The results of the constituent analysis are presented in the next section together with the results of the analysis of the diagonal and non-diagonal sum rules.

4 Numerical analysis

Having the necessary formulae at hand we next describe our numerical analysis of the sum rules and specify our choice of the relevant input parameters. We use the following numerical input values for the condensate contributions [2, 17]

$$\begin{aligned} \langle \bar{q}q \rangle &= -(0.23 \text{ GeV})^3 \quad (\text{quark condensate}), \\ \alpha_S \langle G^2 \rangle &= 0.04 \text{ GeV}^4 \quad (\text{gluon condensate}), \quad \text{and} \\ g_S \langle \bar{q} \sigma_{\mu\nu} G^{\mu\nu} q \rangle &= m_0^2 \langle \bar{q}q \rangle \quad \text{with} \quad m_0^2 = 0.8 \text{ GeV}^2 \quad (\text{mixed quark-gluon condensate}). \end{aligned} \tag{41}$$

There are in general two strategies for the numerical analysis of the QCD sum rules. The first strategy fixes the bound state energy $\bar{\Lambda}$ from the outset by choosing a specific value for the pole mass of the heavy quark and then extracts a value for the residue F . In order to obtain information from the sum rules which is independent of specific input values, we adopt a second strategy, namely to determine both $\bar{\Lambda}$ and F by finding simultaneous stability values for them with respect to the Borel parameter T .

The first step in carrying out the numerical analysis of the sum rules is to find a sum rule “window” for the allowed values of the Borel parameter T . The parameter range of T is constrained by two different physical requirements. The first is that the convergence of the OPE expansion must be secured. We therefore demand that the subleading term in the OPE does not contribute more than 30% of the leading order term. This gives a lower limit for the Borel parameter. The upper limit is determined by the requirement that the contributions from the excited states plus the physical continuum (even after Borel transformation) should not exceed the bound state contribution. This requirement is necessary in order to guarantee that the sum rules are as independent as possible of the model-dependent assumptions concerning the profile of the theoretical spectral density, i.e. the model of the continuum.

The lower limit of E_C is given by the requirement that the indicated window should be kept open. For the rest, E_C is a free floating variable which is only limited by the stability requirements on $\bar{\Lambda}$ and F .

Baryon type state	E_C	$\bar{\Lambda}$	F
Λ_Q (L.O.)	$1.2 \pm 0.1 \text{ GeV}$	$0.77 \pm 0.05 \text{ GeV}$	$0.022 \pm 0.001 \text{ GeV}^3$
Λ_Q (N.L.O.)	$1.1 \pm 0.1 \text{ GeV}$	$0.77 \pm 0.05 \text{ GeV}$	$0.027 \pm 0.002 \text{ GeV}^3$
Σ_Q (L.O.)	$1.4 \pm 0.1 \text{ GeV}$	$0.96 \pm 0.05 \text{ GeV}$	$0.031 \pm 0.002 \text{ GeV}^3$
Σ_Q (N.L.O.)	$1.3 \pm 0.1 \text{ GeV}$	$0.94 \pm 0.05 \text{ GeV}$	$0.038 \pm 0.003 \text{ GeV}^3$

Table 2: Results of the diagonal sum rule analysis for the continuum threshold parameter E_C , the bound state energy $\bar{\Lambda}$, and the residuum F for Λ_Q -type and Σ_Q -type currents, analyzed to leading order (L.O.) as well as next-to-leading order (N.L.O.)

4.1 Diagonal sum rules

Let us briefly recapitulate the results of the numerical analysis of the diagonal sum rules presented in [10]. The above two requirements limit the allowed range for the Borel parameter to $250 \text{ MeV} < T < 400 \text{ MeV}$. The analysis proceeded in two steps. First we analyzed the uncorrected sum rules varying both the continuum threshold and the bound state energy. The criterion for the best choice of these two energies is the stability of the sum rules with regard to the variation of the Borel parameter T . In the second step we included the radiative corrections and again varied both the continuum threshold and the bound state energy to obtain the best sum rules stability. The ratio of the continuum contribution and ground state contribution depends strongly on the Borel parameter T and the continuum threshold energy E_C . Looking e.g. at the sum rule analysis for the Λ_Q -type baryons with QCD corrections, the continuum contribution is about 80% of the ground state contribution for $E_C = 1.1 \text{ GeV}$ and $T = 250 \text{ MeV}$ and then increases with T .

Because of the new specification for the sum rule window we have repeated the diagonal sum rule analysis of [10] allowing for slightly different values of $\bar{\Lambda}$ and F . The outcome of the numerical analysis is practically unaltered. The values for the Λ_Q -type state can be read off from Fig. 3. Fig 3(a) shows the dependence of the bound state energy $\bar{\Lambda}$ on the Borel parameter T and Fig. 3(b) shows the dependence of the residue on T , both for the leading order sum rule. Fig. 3(c) and Fig. 3(d) show the same dependencies for the radiatively corrected sum rules. The same analysis is repeated for the Σ_Q -type states in Fig. 4. The results of the numerical analysis both without and with radiative corrections are given in Table 2.

4.2 Non-diagonal sum rules

In the case of the non-diagonal sum rules, the “window” of permissible values for the Borel parameter is wider than in the diagonal case and it is given by $250 \text{ MeV} < T < 600 \text{ MeV}$. Proceeding in the same manner as in the case of the diagonal sum rule analysis, we obtain best stability values when varying T . The values for the Λ_Q -type state can be read off from Fig. 5, and the values for the Σ_Q -type state can be obtained from Fig. 6. For the Λ_Q -type baryons the stability appears at values of T and E_C where the continuum contribution is about 100%. If we try to decrease this contribution relatively by increasing E_C , the stability in T becomes worse. As can be seen from Fig. 5(a), for e.g. $E_C = 1.3 \text{ GeV}$ the contribution of the continuum is less than 40% on the left hand side, but stability is lost. These considerations show that the relative error of our estimate can be taken to be

Baryon type state	E_C	$\bar{\Lambda}$	F
Λ_Q (L.O.)	$1.0 \pm 0.10 \text{ GeV}$	$0.75 \pm 0.10 \text{ GeV}$	$0.024 \pm 0.002 \text{ GeV}^3$
Λ_Q (N.L.O.)	$1.0 \pm 0.10 \text{ GeV}$	$0.72 \pm 0.10 \text{ GeV}$	$0.032 \pm 0.003 \text{ GeV}^3$
Σ_Q (L.O.)	$1.5 \pm 0.10 \text{ GeV}$	$1.16 \pm 0.10 \text{ GeV}$	$0.045 \pm 0.003 \text{ GeV}^3$
Σ_Q (N.L.O.)	$1.2 \pm 0.10 \text{ GeV}$	$0.94 \pm 0.10 \text{ GeV}$	$0.039 \pm 0.004 \text{ GeV}^3$

Table 3: Results of the non-diagonal sum rule analysis for the continuum threshold parameter E_C , the bound state energy $\bar{\Lambda}$, and the residuum F for Λ_Q -type and Σ_Q -type currents, analyzed to leading order (L.O.) as well as next-to-leading order (N.L.O.)

Baryon type state	E_C	$\bar{\Lambda}$	F
Λ_Q (L.O.)	$1.1 \pm 0.10 \text{ GeV}$	$0.77 \pm 0.10 \text{ GeV}$	$0.034 \pm 0.004 \text{ GeV}^3$
Λ_Q (N.L.O.)	$1.1 \pm 0.10 \text{ GeV}$	$0.77 \pm 0.10 \text{ GeV}$	$0.032 \pm 0.004 \text{ GeV}^3$
Σ_Q (L.O.)	$1.3 \pm 0.10 \text{ GeV}$	$1.03 \pm 0.10 \text{ GeV}$	$0.045 \pm 0.004 \text{ GeV}^3$
Σ_Q (N.L.O.)	$1.2 \pm 0.10 \text{ GeV}$	$0.94 \pm 0.10 \text{ GeV}$	$0.036 \pm 0.004 \text{ GeV}^3$

Table 4: Results of the constituent type mixed sum rule analysis for the continuum threshold parameter E_C , the bound state energy $\bar{\Lambda}$, and the residuum F for Λ_Q -type and Σ_Q -type currents, analyzed to leading order (L.O.) as well as next-to-leading order (N.L.O.)

approximately 10%. The situation for the Σ_Q -type baryons is much better. For example, for the radiatively corrected sum rules the ratio of the continuum and the ground state contribution is 50% for the central value $E_C = 1.2 \text{ GeV}$ and 30% for $E_C = 1.5 \text{ GeV}$ at the left end of the allowed range for the Borel parameter T .

The numerical results are given in Table 3. Assuming relative errors of 10% for the bound state energy and 20% for the residue, the obtained values are in agreement with the results of the analysis of the diagonal sum rules, where the values for the Σ_Q -type baryon are the more reliable one.

4.3 Constituent type mixed sum rules

The use of a constituent type interpolating current $J = (J_1 + J_2)/2$ combines the two sum rule formulas for the diagonal and the non-diagonal case, taking one half of each part. The “window” of permissible values for the Borel parameter T is now given by $300 \text{ MeV} < T < 700 \text{ MeV}$. In Fig. 7 we show the results of the sum rule analysis for the Λ_Q -type baryons, and in Fig. 8 we show the results for the Σ_Q -type baryons.

The numerical results of the analysis are given in Table 4. The constituent type sum rules show an improved stability on the Borel parameter T as compared to the non-diagonal sum rules, but the stability is not as good as in the diagonal case. Within the assumed errors the results are again in agreement with both the diagonal and the non-diagonal sum rule analysis.

4.4 Comparison with experimental values

Finally we want to compare our results for the bound state energy with the existing experimental values for the baryon masses. For such a comparison we need to know the pole mass of the heavy quarks which can be extracted from the heavy quarkonium and heavy-light mesons [18, 19, 20]. The quoted value of the bottom quark pole mass varies from $m_b = 4.55 \pm 0.05 \text{ GeV}$ [19] and $m_b = 4.67 \pm 0.10 \text{ GeV}$ [20] to $m_b = 4.80 \pm 0.03 \text{ GeV}$ [18]. Assuming the range $4.6 \text{ GeV} < m_b < 4.9 \text{ GeV}$, the mass $m(\Lambda_b) = 5642 \pm 50 \text{ MeV}$ of the baryon Λ_b [21] results in a range $740 \text{ MeV} < \bar{\Lambda}(\Lambda_b) < 1040 \text{ MeV}$ for the bound state energy. Our central value $\bar{\Lambda}(\Lambda_Q) = 760 \text{ MeV}$ for the bound state energy suggests a pole mass of $m_b = 4880 \text{ MeV}$ for the bottom quark.

Taking the experimental results for charm-quark baryons, namely $m(\Lambda_c) = 2284.9 \pm 0.6 \text{ MeV}$ and $m(\Sigma_c^+) = 2453.5 \pm 0.9 \text{ MeV}$ [21], our central values $\bar{\Lambda}(\Lambda_Q) = 760 \text{ MeV}$ and $\bar{\Lambda}(\Sigma_Q) = 940 \text{ MeV}$ predict a mean pole mass of $m_c = 1520 \text{ MeV}$ for the charm quark.

5 Conclusions

We have considered the operator product expansion of the correlator of two static heavy baryon currents at small Euclidian distances and determined the α_S radiative corrections to the first and second Wilson coefficient in the expansion. Based on the operator product expansion we have formulated and analyzed heavy baryon sum rules for the Λ_Q -type and Σ_Q -type heavy baryons using two different types of interpolating fields for the baryons in each case. In this paper we have constructed and analyzed the non-diagonal sum rules built from the correlators of two different currents including radiative corrections. The non-diagonal sum rules bring in some new features such as a more “normal” behaviour of the spectral density $\rho(\omega) \approx \langle \bar{q}q \rangle \omega^2$ and moderate QCD corrections to the spectral density as compared to the diagonal case. We have taken a second look at the diagonal sum rules.

We have also set up and analyzed constituent type heavy baryon sum rules where we have used interpolating currents that are expected to have a maximum overlap with the heavy baryon’s light diquark system in the constituent quark model picture. All the three types of sum rules show acceptable stability in their dependence on the Borel parameter, where the best stability was obtained for the diagonal sum rules. The results of the three types of sum rules (diagonal, non-diagonal, constituent type) on the bound state energy and the residues of the heavy ground state baryons were found to be consistent with each other, where the values obtained for the Σ_Q -type baryons are more reliable than the results for the Λ_Q -type baryons.

Acknowledgments:

This work was partially supported by the BMBF, FRG, under contract 06MZ865, and by the Human Capital and Mobility program under contract CHRX-CT94-0579. The work of O.I.Y. was supported by the BMBF, FRG, under contract 057WZ91P(0). We would like to thank A. Grozin, B. Tausk and A. Khodjamirian for valuable discussions.

Appendix

In this appendix we collect our results on the evaluation of the one-loop and two-loop contributions to the non-diagonal correlators of two heavy baryon currents. The contributing diagrams are shown in Fig. 2. Introducing the abbreviation $E_n = \Gamma(1-\epsilon)^n \Gamma(1+n\epsilon)$ (with integer numbers $n = 1, 2, 3, \dots$) we obtain

$$D_0 = \frac{4\tilde{\Gamma}_0 E_1}{(D-4)(D-3)}, \quad D_1 = D_2 = \frac{2(D-2)\tilde{\Gamma}_0 E_2}{(D-4)^2(D-3)(2D-7)}, \quad (\text{A1})$$

$$D_3 = \frac{8(D-2)\tilde{\Gamma}_0 E_1^2}{(D-4)^3(D-3)^2} - \frac{4(D-2)(3D-10)\tilde{\Gamma}_0 E_2}{(D-4)^3(D-3)^2(2D-7)}, \quad (\text{A2})$$

$$D_4 = \frac{(D-4)\tilde{\Gamma}_1 + \tilde{\Gamma}_2}{(D-4)^2(D-3)(2D-7)} E_2, \quad D_5 = \frac{2(D-2)\tilde{\Gamma}_0 - D\tilde{\Gamma}_1 + \tilde{\Gamma}_2}{(D-4)^2(D-3)(2D-7)} E_2, \quad (\text{A3})$$

$$D_6 = \frac{2D(D-2)\tilde{\Gamma}_0 E_2}{(D-4)^2(D-3)(2D-7)}, \quad D_7 = \frac{2(D-2)\tilde{\Gamma}_0 E_2}{(D-4)^2(D-3)(2D-7)}, \quad (\text{A4})$$

$$D_8 = \frac{-4(D-2)\tilde{\Gamma}_0 E_2}{(D-4)^2(D-3)^2(2D-7)} \quad (\text{A5})$$

where $\tilde{\Gamma}_0 = \text{Tr}(\bar{\Gamma}\psi\Gamma\psi)$, $\tilde{\Gamma}_1 = \text{Tr}(\bar{\Gamma}\gamma_\mu\Gamma\gamma^\mu)$, and $\tilde{\Gamma}_2 = \text{Tr}(\bar{\Gamma}\psi\gamma_\mu\gamma_\nu\Gamma\gamma^\nu\gamma^\mu\psi)$.

References

- [1] M. Neubert, ‘‘Heavy Quark Symmetry’’, Phys. Rep. **245** (1994) 259
- [2] M.A. Shifman, A.I. Vainshtein and V.I. Zakharov, Nucl. Phys. **B147** (1979) 385; **B147** (1979) 448
- [3] E.V. Shuryak, Nucl. Phys. **B198** (1982) 83
- [4] A.G. Grozin and O.I. Yakovlev, Phys. Lett. **285 B** (1992) 254
- [5] E. Bagan, M. Chabab, H.G. Dosch and S. Narison, Phys. Lett. **301 B** (1993) 243
- [6] V.M. Belyaev and B.Y. Blok, Z. Phys. **C30** (1986) 151; B.Y. Blok and V.L. Eletzky, Z. Phys. **C30** (1986) 229
- [7] E. Bagan, M. Chabab, H.G. Dosch and S. Narison, Phys. Lett. **278 B** (1992) 367; **287 B** (1992) 176
- [8] V.L. Chernyak and I.R. Zhitnitsky, Nucl. Phys. **B246** (1984) 52; V.L. Chernyak, A.A. Ogloblin and I.R. Zhitnitsky, Z. Phys. **C42** (1989) 569
- [9] S. Groote, J.G. Körner and O.I. Yakovlev, Phys. Rev. **D54** (1996) 3447
- [10] S. Groote, J.G. Körner and O.I. Yakovlev, Phys. Rev. **D55** (1997) 3016

- [11] D. Broadhurst, A.G. Grozin, Phys. Lett. **274 B** (1992) 421
- [12] E. Bagan, P. Ball, V.M. Braun and H.G. Dosch, Phys. Lett. **278 B** (1992) 457
- [13] W.A. Bardeen, A.J. Buras, D.W. Duke and T. Muta, Phys. Rev. **D18** (1978) 3998
- [14] X. Ji and M.J. Musolf, Phys. Lett. **257 B** (1991) 409
- [15] D.J. Broadhurst and A.G. Grozin, Phys. Lett. **267 B** (1991) 105
- [16] E. Witten, Nucl. Phys. **B223** (1983) 483;
 C. Carone, H. Georgi and S. Osofski, Phys. Lett. **332 B** (1994) 483;
 M. Luty and J. March-Russel, Nucl. Phys. **B246** (1994) 71;
 R.F. Dashen, E. Jenkins and A.V. Manohar, Phys. Rev. **D49** (1994) 4713;
 Phys. Rev. **D51** (1995) 3697
- [17] S. Narison, “QCD Sum Rules”, World Scientific, Singapore, 1989
- [18] M.B. Voloshin and Y.M. Zaitsev, Sov. Phys. Usp. **30** (1987) 553
- [19] L.J. Reinders, Phys. Rev. **D38** (1988) 947
- [20] S. Narison, Phys. Lett. **197 B** (1987) 405
- [21] Particle Data Group, R.M. Barnett *et al*, Phys. Rev. **D50** (1996) 1

Figure Captions

- Fig. 1: Radiative corrections to the diagonal correlator. (0) lowest order two-loop contribution, (1)–(4) $O(\alpha_S)$ three-loop contributions.
- Fig. 2: Radiative corrections to the non-diagonal correlator given by the dimension three condensate contribution. (0) lowest order one-loop contribution, (1)–(8) $O(\alpha_S)$ two-loop contributions.
- Fig. 3: Bound state energy and residue of the Λ_Q as functions of the Borel parameter T (diagonal case). Plotted are five curves for five different values of the threshold energy E_C spaced by 100 MeV around the central value $E_C = E_C^{\text{best}}$. E_C increases from bottom to top.
 - (a) lowest order sum rule results for the bound state energy $\bar{\Lambda}(\Lambda)$
 - (b) lowest order sum rule results for the residue F_Λ
 - (c) $O(\alpha_S)$ sum rule results for the bound state energy $\bar{\Lambda}(\Lambda)$ for the current $J_{\Lambda 1}$
 - (d) $O(\alpha_S)$ sum rule results for the residue F_Λ for the current $J_{\Lambda 1}$
- Fig. 4: Bound state energy and residue of the Σ_Q as functions of the Borel parameter T (diagonal case). Plotted are five curves for five different values of the threshold energy E_C spaced by 100 MeV around the central value $E_C = E_C^{\text{best}}$. E_C increases from bottom to top.

- (a) lowest order sum rule results for the bound state energy $\bar{\Lambda}(\Sigma)$
- (b) lowest order sum rule results for the residue F_Σ
- (c) $O(\alpha_S)$ sum rule results for the bound state energy $\bar{\Lambda}(\Sigma)$ for the current $J_{\Sigma 1}$
- (d) $O(\alpha_S)$ sum rule results for the residue F_Σ for the current $J_{\Sigma 1}$

Fig. 5: Bound state energy and residue of the Λ_Q as functions of the Borel parameter T (non-diagonal case). Plotted are five curves for five different values of the threshold energy E_C spaced by 100 MeV around the central value $E_C = E_C^{\text{best}}$. E_C increases from bottom to top.

- (a) lowest order sum rule results for the bound state energy $\bar{\Lambda}(\Lambda)$
- (b) lowest order sum rule results for the residue F_Λ
- (c) $O(\alpha_S)$ sum rule results for the bound state energy $\bar{\Lambda}(\Lambda)$ for the two currents $J_{\Lambda 1}$ and $J_{\Lambda 2}$
- (d) $O(\alpha_S)$ sum rule results for the residue F_Λ for the two currents $J_{\Lambda 1}$ and $J_{\Lambda 2}$

Fig. 6: Bound state energy and residue of the Σ_Q as functions of the Borel parameter T (non-diagonal case). Plotted are five curves for five different values of the threshold energy E_C spaced by 100 MeV around the central value $E_C = E_C^{\text{best}}$. E_C increases from bottom to top.

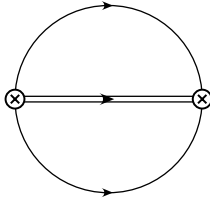
- (a) lowest order sum rule results for the bound state energy $\bar{\Lambda}(\Sigma)$
- (b) lowest order sum rule results for the residue F_Σ
- (c) $O(\alpha_S)$ sum rule results for the bound state energy $\bar{\Lambda}(\Sigma)$ for the two currents $J_{\Sigma 1}$ and $J_{\Sigma 2}$
- (d) $O(\alpha_S)$ sum rule results for the residue F_Σ for the two currents $J_{\Sigma 1}$ and $J_{\Sigma 2}$

Fig. 7: Bound state energy and residue of the Λ_Q as functions of the Borel parameter T (constituent type mixed case). Plotted are five curves for five different values of the threshold energy E_C spaced by 100 MeV around the central value $E_C = E_C^{\text{best}}$. E_C increases from bottom to top.

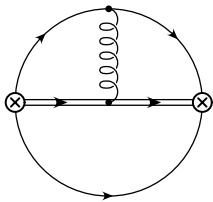
- (a) lowest order sum rule results for the bound state energy $\bar{\Lambda}(\Lambda)$
- (b) lowest order sum rule results for the residue F_Λ
- (c) $O(\alpha_S)$ sum rule results for the bound state energy $\bar{\Lambda}(\Lambda)$ for the two currents $J_{\Lambda 1}$ and $J_{\Lambda 2}$
- (d) $O(\alpha_S)$ sum rule results for the residue F_Λ for the two currents $J_{\Lambda 1}$ and $J_{\Lambda 2}$

Fig. 8: Bound state energy and residue of the Σ_Q as functions of the Borel parameter T (constituent type mixed case). Plotted are five curves for five different values of the threshold energy E_C spaced by 100 MeV around the central value $E_C = E_C^{\text{best}}$. E_C increases from bottom to top.

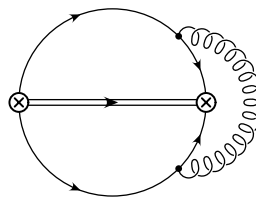
- (a) lowest order sum rule results for the bound state energy $\bar{\Lambda}(\Sigma)$
- (b) lowest order sum rule results for the residue F_Σ
- (c) $O(\alpha_S)$ sum rule results for the bound state energy $\bar{\Lambda}(\Sigma)$ for the two currents $J_{\Sigma 1}$ and $J_{\Sigma 2}$
- (d) $O(\alpha_S)$ sum rule results for the residue F_Σ for the two currents $J_{\Sigma 1}$ and $J_{\Sigma 2}$



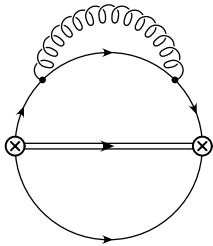
(0)



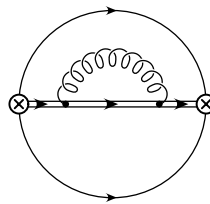
(1)



(2)

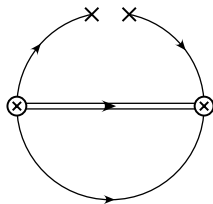


(3)

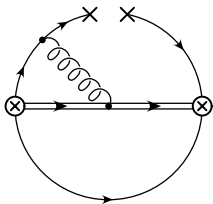


(4)

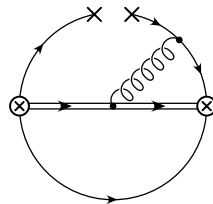
Figure 1



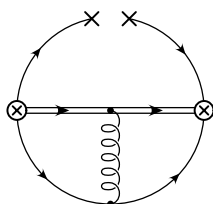
(0)



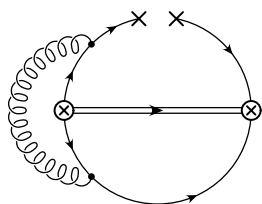
(1)



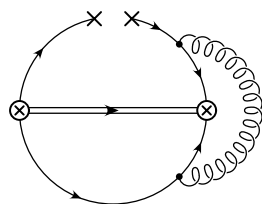
(2)



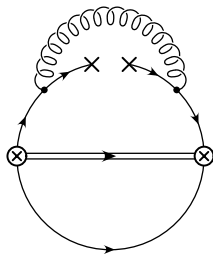
(3)



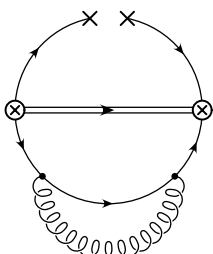
(4)



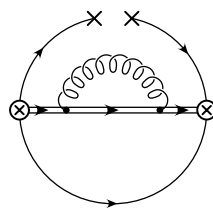
(5)



(6)

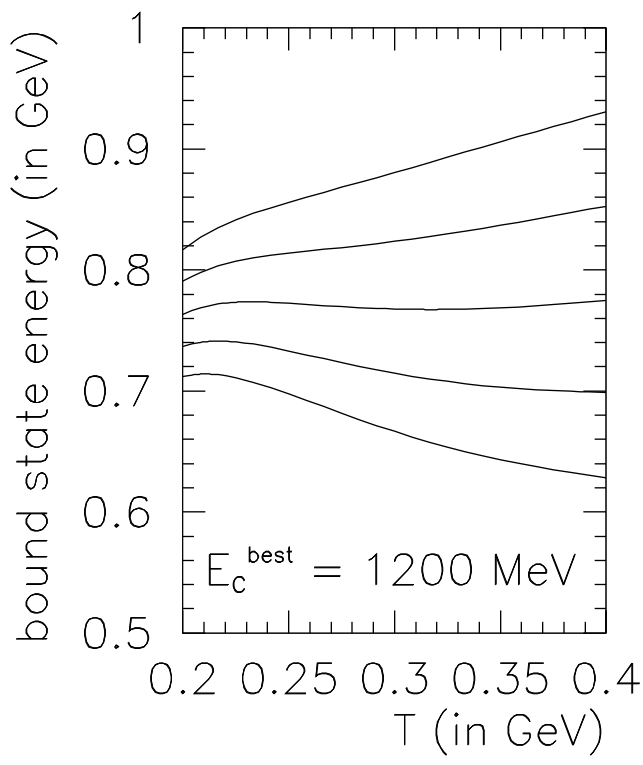


(7)

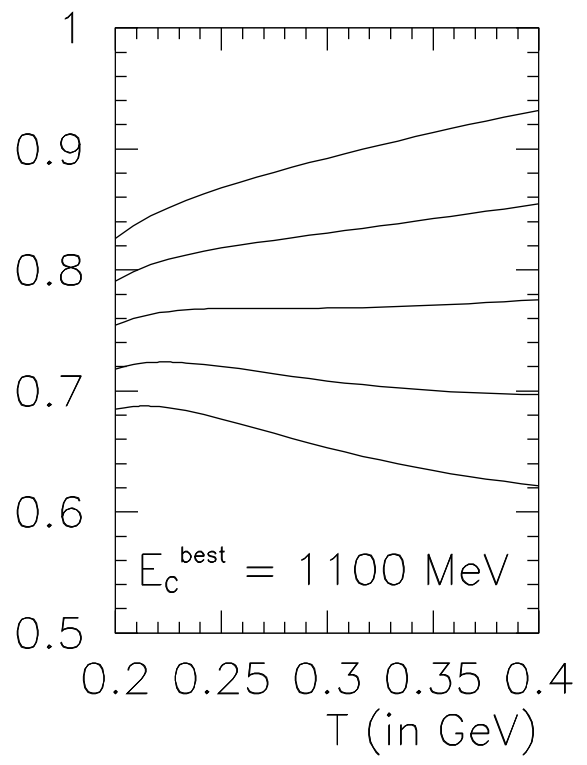


(8)

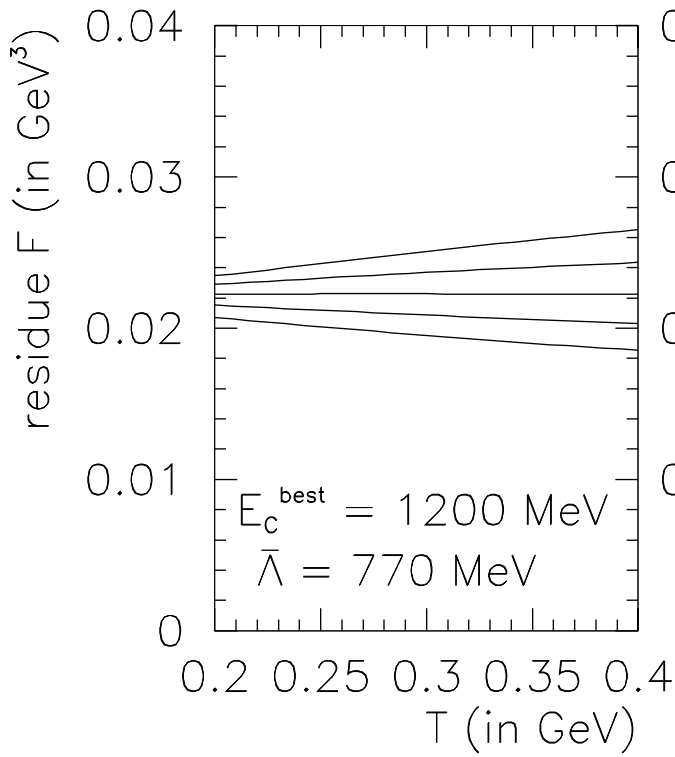
Figure 2



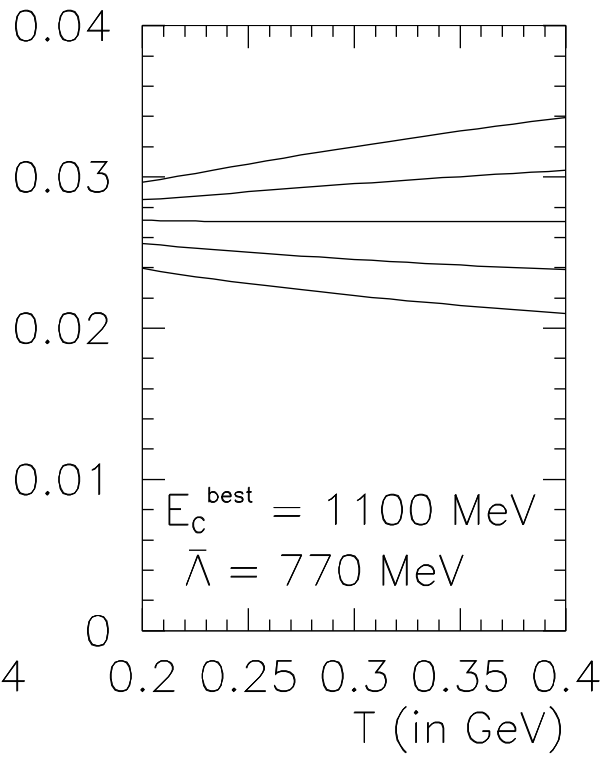
(a)



(c)

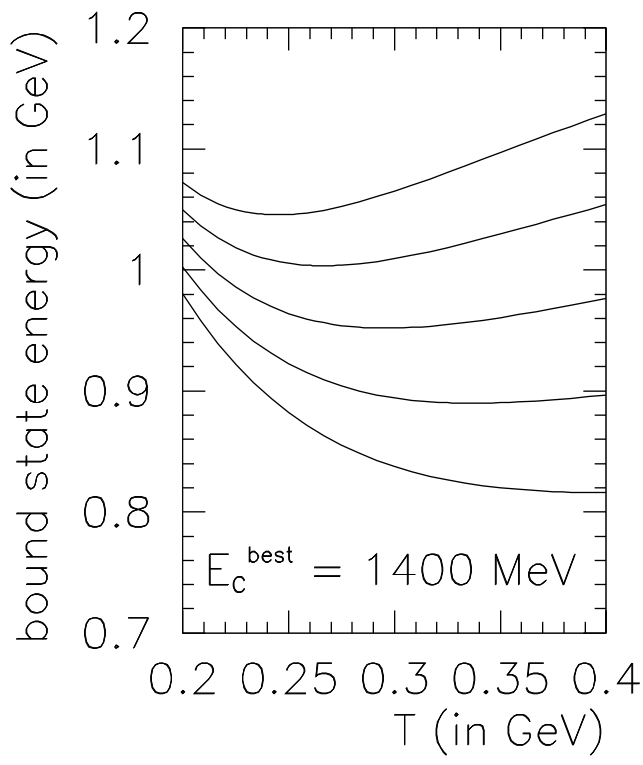


(b)

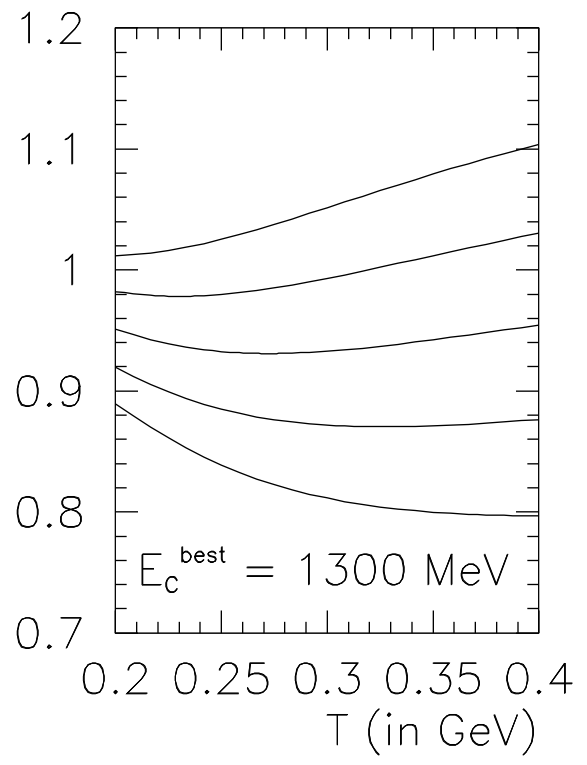


(d)

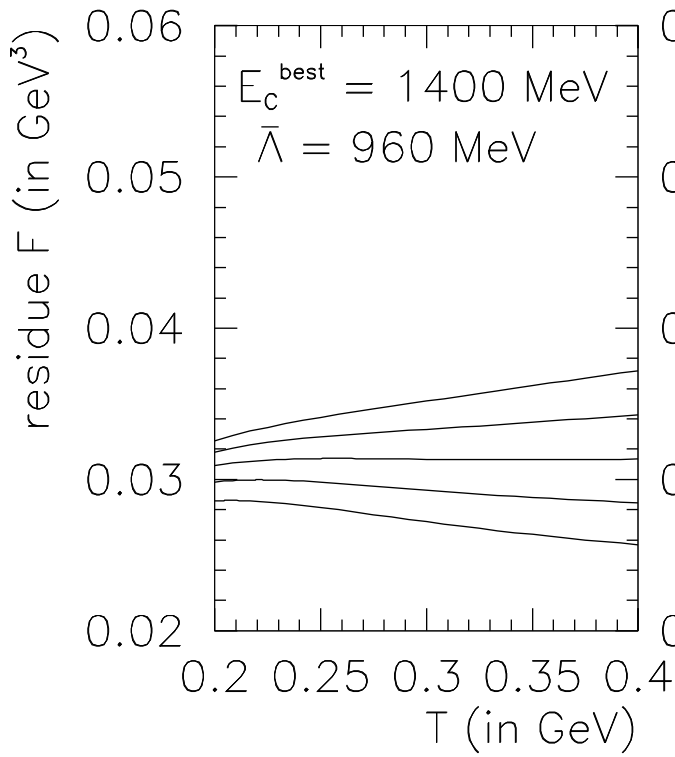
Figure 3



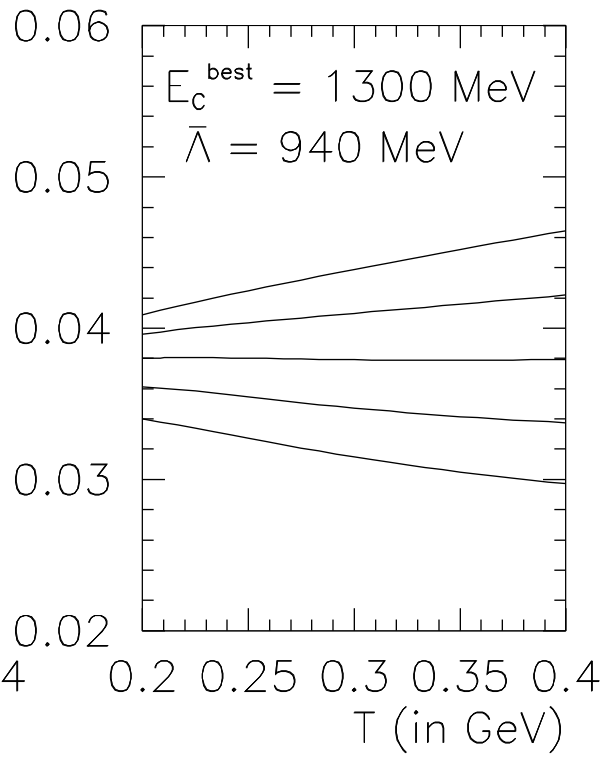
(a)



(c)

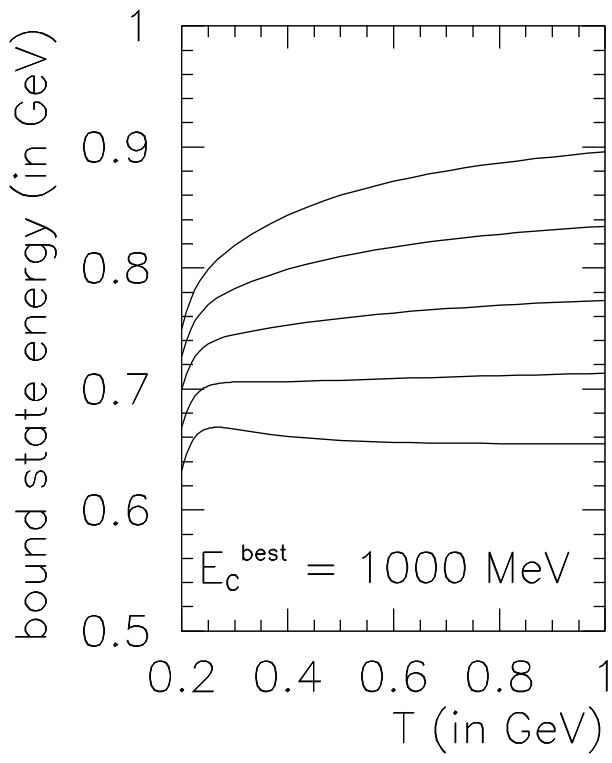


(b)

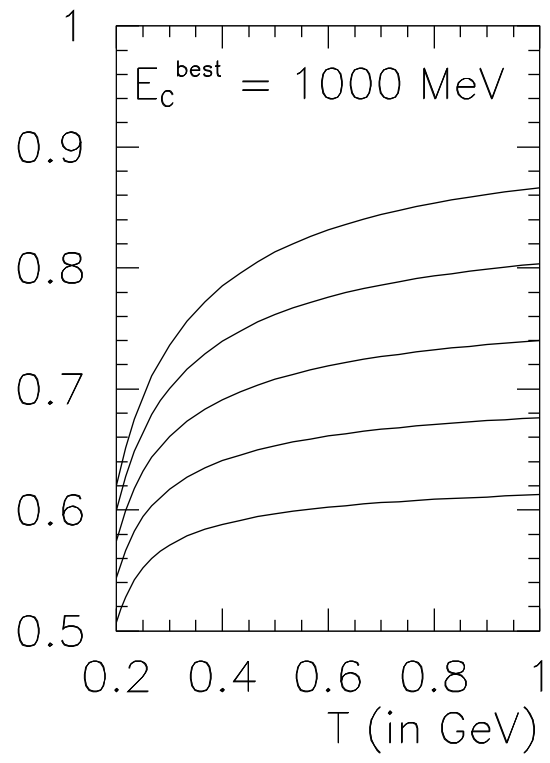


(d)

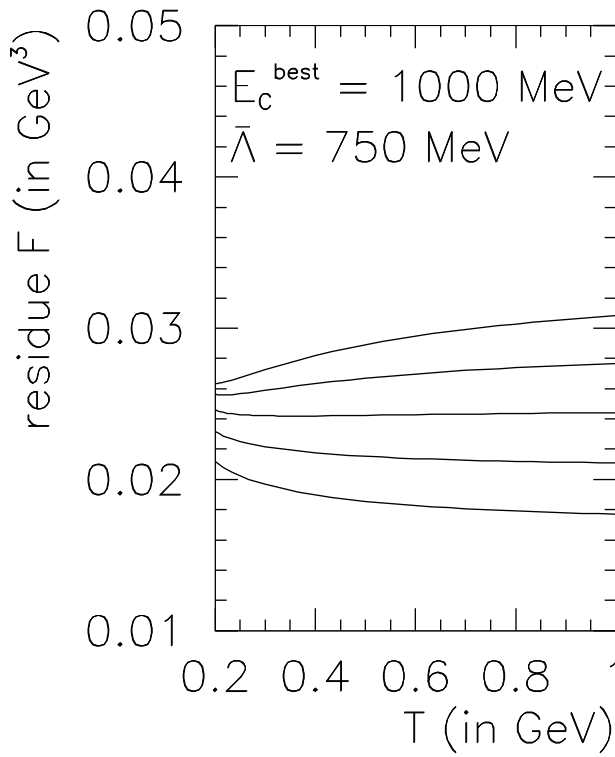
Figure 4



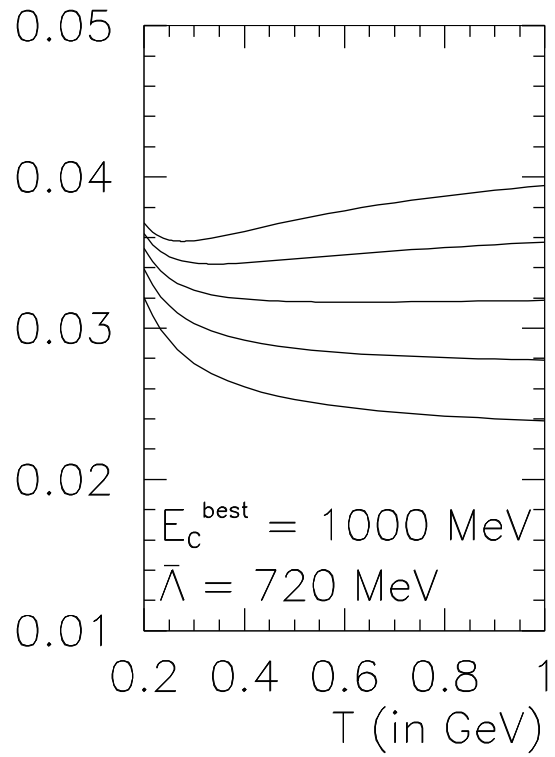
(a)



(c)

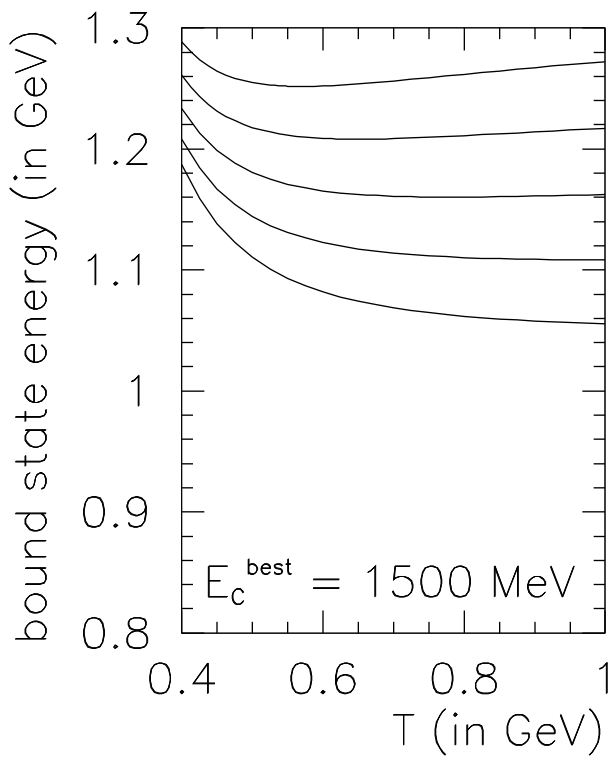


(b)

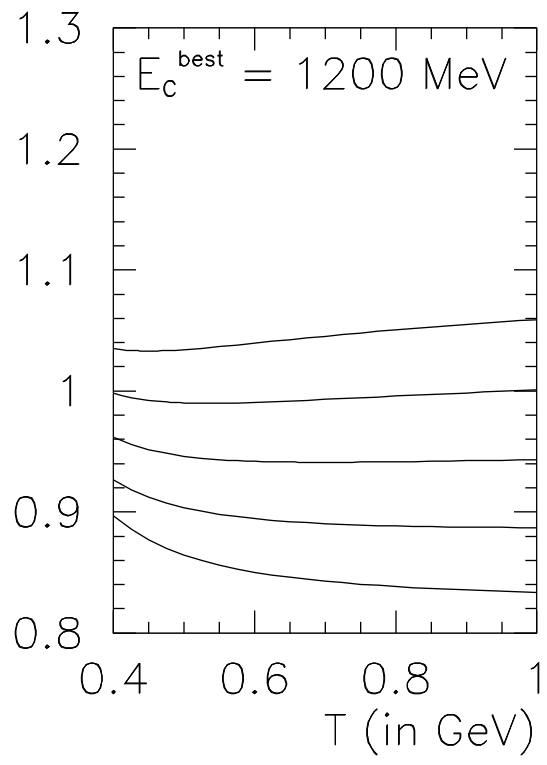


(d)

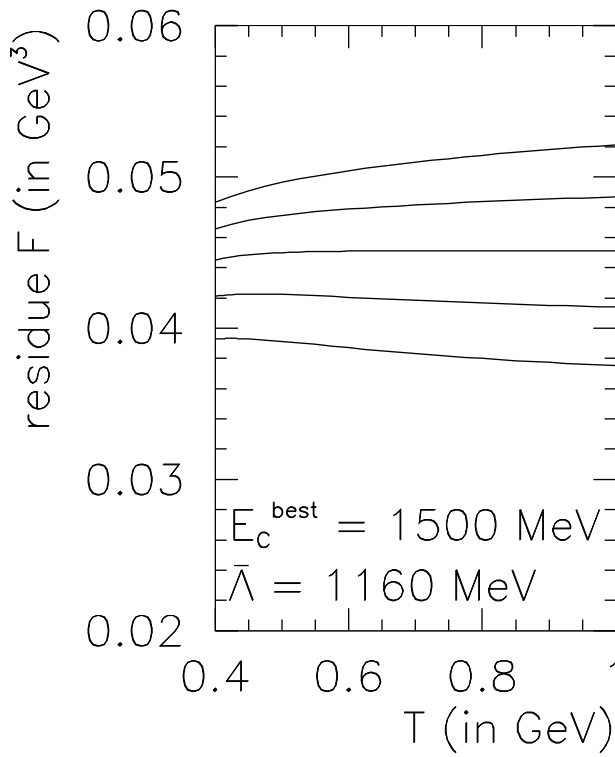
Figure 5



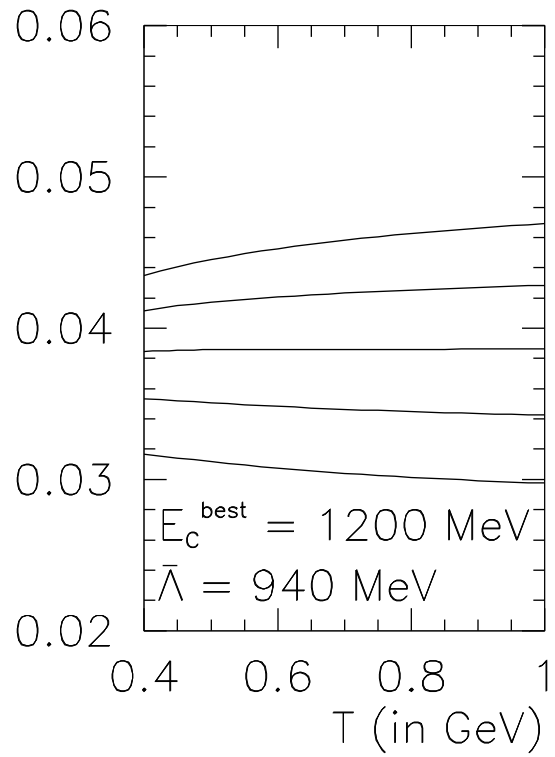
(a)



(c)

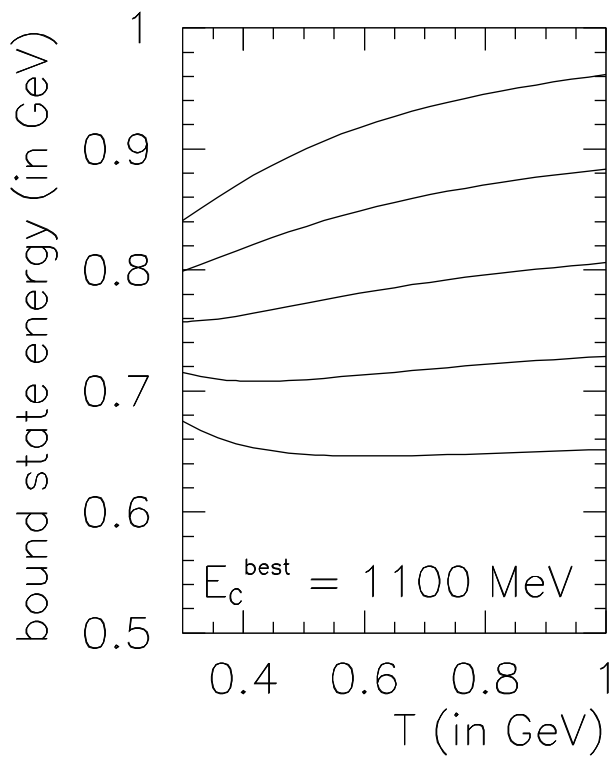


(b)

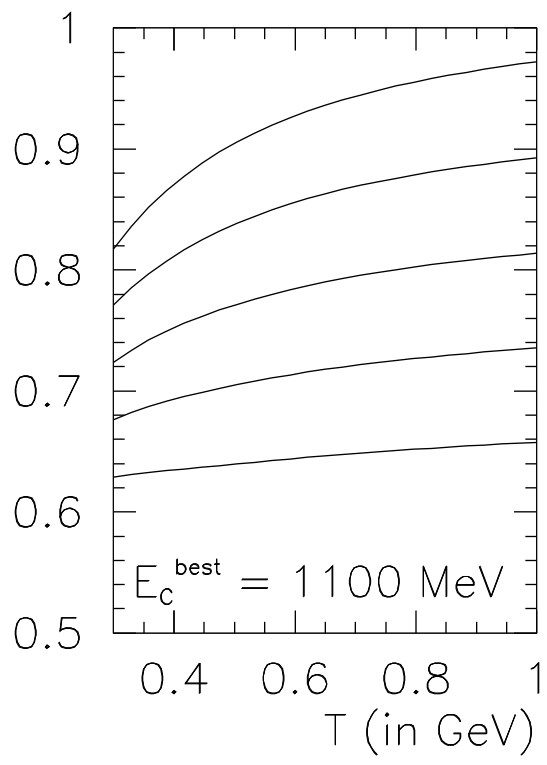


(d)

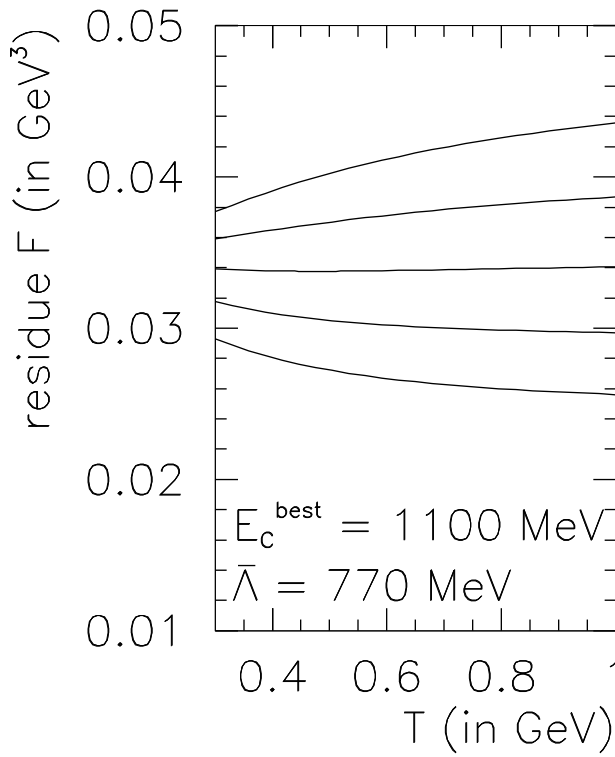
Figure 6



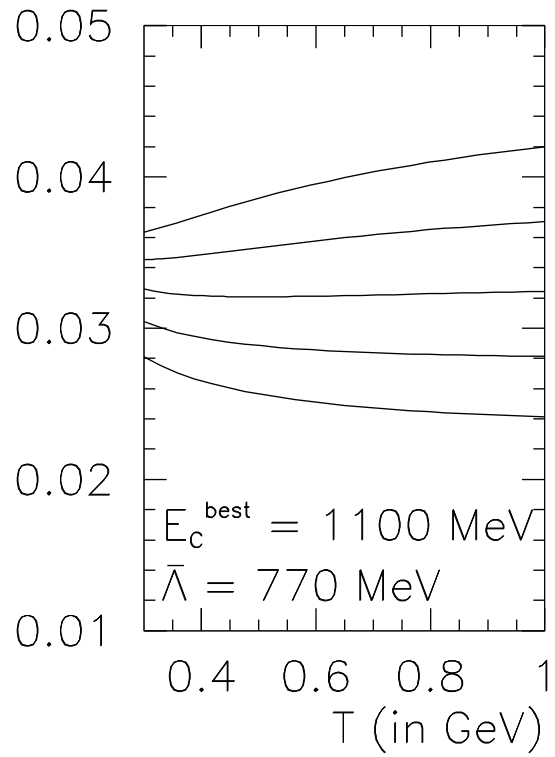
(a)



(c)

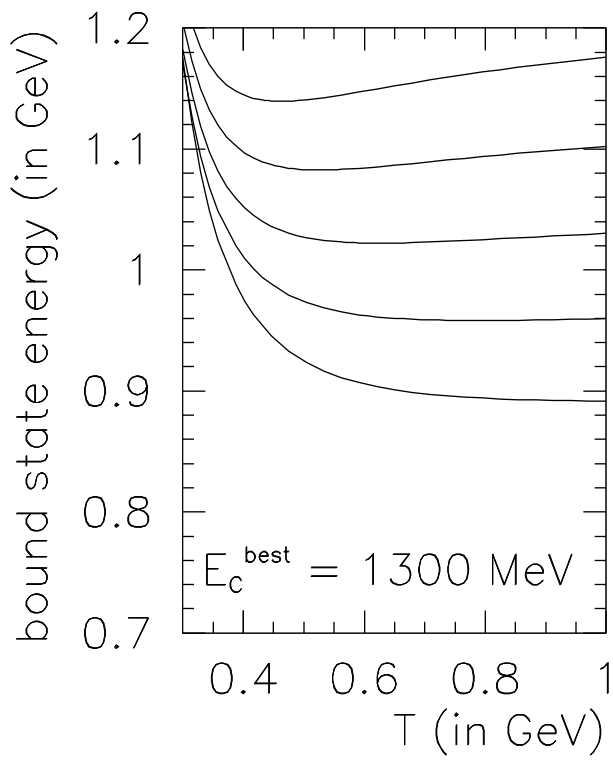


(b)

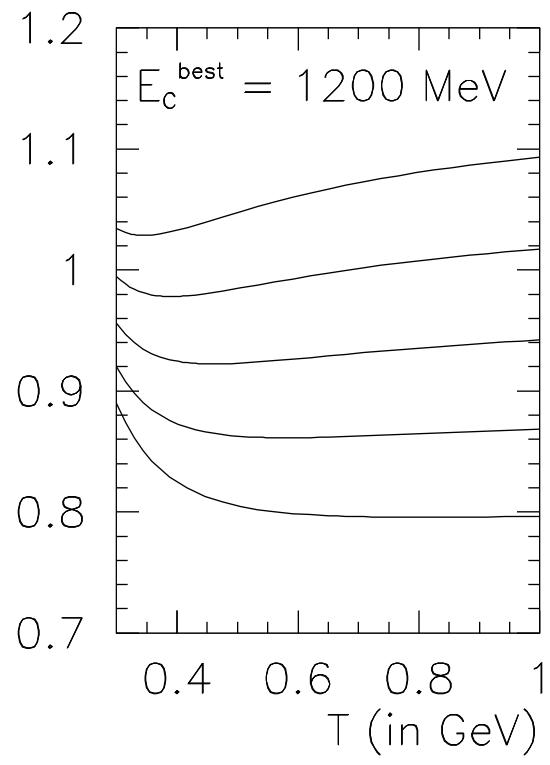


(d)

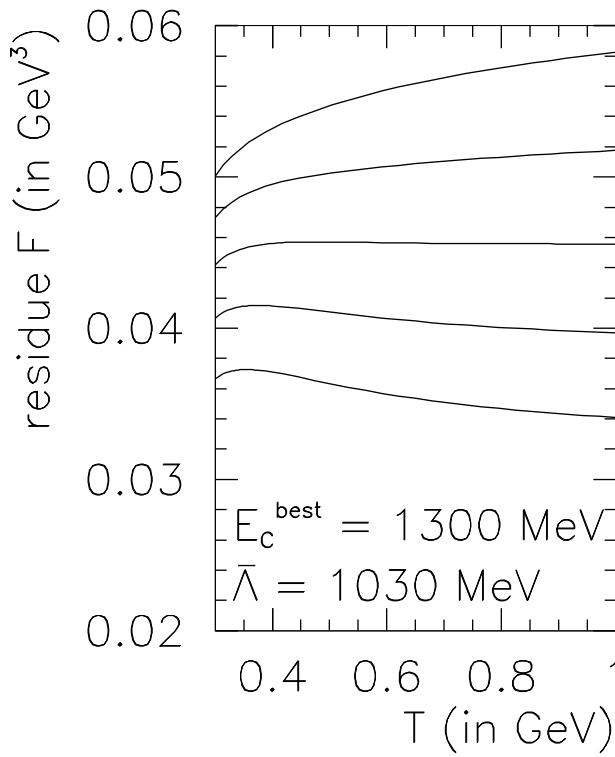
Figure 7



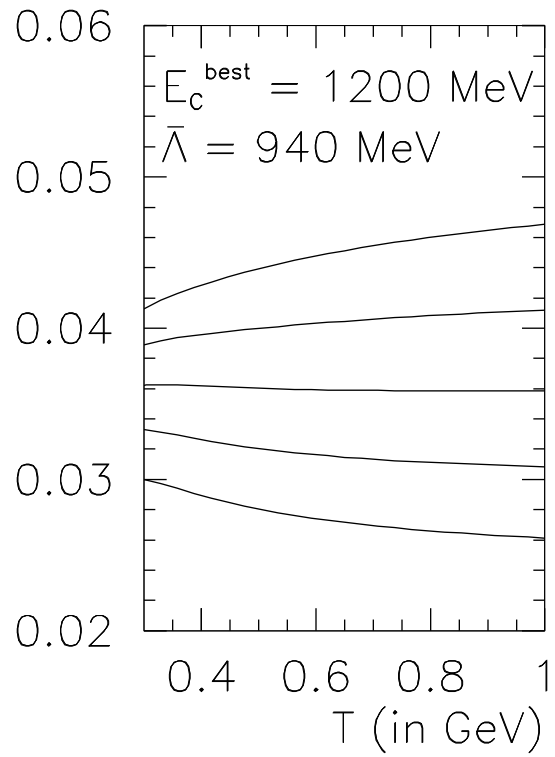
(a)



(c)



(b)



(d)

Figure 8